

*Full Paper***Electrochemical Determination of Ciprofloxacin  
Using Glassy Carbon Electrode Modified with  
CoFe<sub>2</sub>O<sub>4</sub>-MWCNT****Asieh Hosseini,<sup>1</sup> Esmail Sohoul, <sup>2</sup> Maryam Gholami,<sup>3</sup> Ali Sobhani-Nasab<sup>4,5,\*</sup> and  
Seyed Ali Mirhosseini<sup>6</sup>**<sup>1</sup>*Razi Drug Research Center, Iran University of Medical Sciences, Tehran, Iran*<sup>2</sup>*Young Researchers and Elites club, Science and Research Branch, Islamic Azad University, Tehran, Iran*<sup>3</sup>*Department of Chemistry, Azad University-North Tehran Branch, Tehran, Iran*<sup>4</sup>*Social Determinants of Health (SDH) Research Center, Kashan University of Medical Sciences, Kashan, Iran*<sup>5</sup>*Core Research Lab, Kashan University of Medical Sciences, Kashan, Iran*<sup>6</sup>*Applied Microbiology Research Center, Systems Biology and Poisonings Institute, Baqiyatallah University of Medical Sciences, Tehran, Iran*

\*Corresponding Author, Tel.: +982182482584; Fax: +9821 88068924

E-Mail: [Ali.sobhaninasab@gmail.com](mailto:Ali.sobhaninasab@gmail.com)*Received: 6 June 2019 / Received in revised form: 26 July 2019 /**Accepted: 30 July 2019 / Published online: 31 August 2019*

---

**Abstract-** CoFe<sub>2</sub>O<sub>4</sub> nanostructures composed of spherical-like were obtained by sol-gel method with glucose as template and combine with MWCNT and composed CoFe<sub>2</sub>O<sub>4</sub>-MWCNT heterostructure. The crystal Structure, phase composition, morphology and magnetic properties of CoFe<sub>2</sub>O<sub>4</sub>/MWCNT heterostructure were characterized by X-ray diffraction (XRD), scanning electron microscopy (SEM), and vibrating sample magnetometers (VSM), A pure phase of well crystallized CoFe<sub>2</sub>O<sub>4</sub> nanostructures, with average size of 60 nm, could be readily synthesized at present glucose. The modified glassy carbon (GC) electrode with CoFe<sub>2</sub>O<sub>4</sub>-MWCNT heterostructure was used to determine the ciprofloxacin concentration. A cyclic voltammetric technique was used for comparison between the unmodified and modified electrodes. The fabricated modified electrode shows linear response for detection of ciprofloxacin at two linear range of 0.1-1 μM and 1-30 μM with a detection limit of 0.036 μM.

**Keywords-** Ciprofloxacin, Electrochemical Determination, Glassy Carbon Electrode, CoFe<sub>2</sub>O<sub>4</sub>/MWCNT, Sol-gel method

---

## 1. INTRODUCTION

Nanomaterials with specific characteristics reveal interesting and new behaviors supported such as size and morphology. Recently nanotechnology has developed the different field. Such developments have led to obtained of Nanomaterials with particular morphology and size. Nanomaterials with modern application is on the rise. Through modern and new process, we are able to comprehend various fields including biology physic and chemistry much to a great extent. Therefore, this success has come with making use of nanomaterials in our daily life [1-15].  $\text{MFe}_2\text{O}_4$ , has been extensively studied for its usage as anodes (its theoretical capacity is  $895 \text{ mA h g}^{-1}$ ), semiconductors, sensors, crystals, and magnetic materials. This composition has two structures, cubic and tetragonal, which depends on preparation condition [16-19]. It has been confirmed that,  $\text{MFe}_2\text{O}_4$  has considerable catalytic activity and can be prepared through chemical, combustion, co-precipitation and Microwave hydrothermal method [20, 22].

Nevertheless, its electrical disconnection from current collector and sever electrode pulverization, result in low cycling stability and fast rapid capacity fading. Moreover, the natural poor conductivity of the  $\text{MFe}_2\text{O}_4$  electrode can be considered as a negative factor to negatively affect its application. Graphite is one of the allotropes of carbon, which has been widely employed to obtain different hybrid materials. In addition, it has distinctive ultra-thin structure, noticeable specific area, great mechanical flexibility, and high electrode conductivity [23]. The application of metal oxide composites containing graphite as anode materials have been widely studies. The enhanced electrochemical performance stems from the synergistic effect between transition metal oxides and graphite. In these systems, the graphite sheets use as not only a conductive network to make easy electron transport and lithium ion diffusion of anchored host materials, but also a structural buffer to keep the structural integrity of the electrode in the cycling procedure [24]. Besides, it has been shown that the nanosized material incorporated into electron material can operate as an economic and encouraging way to increase the conductivity and stop the aggregation of active materials in discharge/charge process [25, 26].

Among the reported methods, the sol-gel process is an efficient and economical way to mass production of ultrafine  $\text{CoFe}_2\text{O}_4$  powder.

Ciprofloxacin is a fluoroquinolone antibiotic, with chemical name of 1-cyclopropyl-6-fluoro-4-oxo-7-(piperazine-1-yl) quinoline-3-carboxylic acid. One of the most important antibiotics approved by the Food and Drug Administration which are used to treat infections caused by various bacteria and those who are infected with anthrax [27]. So far, various methods such as chromatography [28] have been used to analyze this drug, however, electrochemical methods have also been developed for this drug in recent years. Among the electrochemical sensors that have been reported for this drug, are boron-doped diamond electrode [27], DNA-GC electrode, MWCNT/GC electrode and etc. [29]. The widespread use

of electrochemical methods to determine the electroactive species [30-38] and different compounds has not prevented the preparation of electrochemical sensors for this drug. In this work,  $\text{CoFe}_2\text{O}_4$  spherical-like nanostructures were synthesized by the sol-gel process with green, nontoxic and new capping agent. Then composited  $\text{CoFe}_2\text{O}_4$  with MWCNT in surface electrode. The obtained samples were characterized by SEM, XRD, VSM, and FT-IR. Vibration samples magnetic showed a magnetization saturation ( $M_s$ ) was 5 emu/g with coercivity ( $H_c$ ) of 2000 Oe for  $\text{CoFe}_2\text{O}_4/\text{MWCNT}$  heterostructure.

## 2. EXPERIMENTAL

### 2.1. Materials and experiments

The phase compositions and structures of the  $\text{CoFe}_2\text{O}_4$  and  $\text{CoFe}_2\text{O}_4/\text{MWCNT}$  heterostructure were determined by X-ray diffraction analyzer with  $\text{Cu-K}\alpha$  radiation ( $\lambda=0.15418$  nm) over the  $2\theta$  range of  $10-80^\circ$  using Rigaku D-max C III, X-ray diffractometer (XRD). The morphology of the  $\text{CoFe}_2\text{O}_4/\text{MWCNT}$  heterostructure was determined using. The morphology of the heterostructure was determined using KYKY-EM3200 Scanning Electron Microscopy (SEM). The magnetic properties of the samples were detected at room temperature using a vibrating sample magnetometer (VSM, Meghnatis Kavir Kasha Co. Kasha, Iran). FT-IR spectrum of  $\text{CoFe}_2\text{O}_4$  has been achieved with Shimadzu Varian 4300 spectrophotometer. The EM-STATE 3+ PALM SENSE Potentiostat Device equipped with the three-electrode system including the  $\text{Ag}/\text{AgCl}$  reference electrode, platinum wire auxiliary electrodes, and glassy carbon electrode was used for electrochemical testing. The Briton Robinson buffer was prepared by mixing the phosphoric acid, acetic acid, and 0.4 molar boric acid which reached the desired pH with 2 M NaOH solution.

### 2.2. Synthesis of $\text{CoFe}_2\text{O}_4$ nanoparticles

$\text{Co}(\text{NO}_3)_2 \cdot 6\text{H}_2\text{O}$  and  $\text{Fe}(\text{NO}_3)_3 \cdot 9\text{H}_2\text{O}$  and glucose were used as starting materials.  $\text{CuFe}_2\text{O}_4$  nanoparticles were prepared by reaction between  $\text{Co}(\text{NO}_3)_2 \cdot 6\text{H}_2\text{O}$  and  $\text{Fe}(\text{NO}_3)_3 \cdot 9\text{H}_2\text{O}$  with molar ratio of 1:2. At first, 1 mmol of  $\text{Co}(\text{NO}_3)_2 \cdot 6\text{H}_2\text{O}$  was dissolved in 50 ml of distilled water, and then an aqueous solution including a stoichiometric amount of  $\text{Fe}(\text{NO}_3)_3 \cdot 9\text{H}_2\text{O}$  dissolved in an equal volume of distilled water was added into the above solution dropwise and the solution was kept vigorously stirred at  $60^\circ\text{C}$  for 20 min. Then, 3 mmol of  $\text{NH}_3$  was dissolved with a minimum amount of de-ionized water and was added to above solution (pH=12) for achieving to pure phase of product. Followed by, thermal dehydration executed and heating was holding until created gel expanded due to auto combustion reaction. The derived powder this reaction disinterred at  $800^\circ\text{C}$ .

### 2.3. Synthesis of CoFe<sub>2</sub>O<sub>4</sub>/MWCNT heterostructure

The CoFe<sub>2</sub>O<sub>4</sub> nanostructure, were obtained through dispersing desired quantities of the nanostructures CoFe<sub>2</sub>O<sub>4</sub> in 50 mL of the water under sonication at 180 W for 20 min. Then, up to a 50 %Wt mixture of the MWCNT were added to the dispersions under sonication at 180 W for 20 min.

### 2.4. Preparation of modified electrode

To prepare the modified glassy carbon electrode for use in the experiments, firstly, the electrode was polished with alumina slurry and washed with distilled water and ethanol to remove any disturbing materials from the surface. The electrode was then placed in 0.5 molar sulfuric acid solutions and the potential scan was applied in the range of 1 to -1 volt to clean the electrode. 2 mg of synthesized nanocomposite was dispersed into 10 mL distilled water, and then 2  $\mu$ L of it was placed on a cleaned glassy carbon electrode using a sampler. The electrode then placed in the oven at 50 ° C to dry, and the CoFe<sub>2</sub>O<sub>4</sub>-MWCNT electrode was prepared. The MWCNT/GC electrode was also prepared in the same way.

## 3. RESULTS AND DISCUSSION

### 3.1. Characterization

Generally, X-ray analysis is being extensively used in research for obtaining the purity and crystal structure of nanoparticles [39-45]. XRD pattern of CoFe<sub>2</sub>O<sub>4</sub> and CoFe<sub>2</sub>O<sub>4</sub>/MWCNT heterostructure is shown in Fig. 1a and b. Fig. 1a confirms XRD pattern relative to pure phase CoFe<sub>2</sub>O<sub>4</sub>. The spectrum of bare CoFe<sub>2</sub>O<sub>4</sub> shows a series of diffraction peaks at the position of 29.68°, 35.89°, and 62.32° with lines (202), (311), and (404), respectively which is in good agreement with JCPDS 34-0425. As well as show, XRD pattern confirms presence of both tetragonal phase of CoFe<sub>2</sub>O<sub>4</sub> (JCPDS No. 34-0425, space group: I41/amd and calculated cell parameters of a=b=5.8444 Å and c=8.6304 Å) and MWCNT. Also, XRD pattern shows formation of CoFe<sub>2</sub>O<sub>4</sub> and CoFe<sub>2</sub>O<sub>4</sub>/MWCNT heterostructure without impurity (Fig. 1b). Crystalline sizes is calculated from Scherrer equation,  $D_c = K\lambda/\beta\cos\theta$ , where  $\beta$  is the width of the observed diffraction peak at its half maximum intensity (FWHM), K is the shape factor, which takes a value of about 0.9, and  $\lambda$  is the X-ray wavelength (Cu K $\alpha$  radiation, equals to 0.154 nm) were about 18 nm for CoFe<sub>2</sub>O<sub>4</sub>/MWCNT nanocomposite [46-53].

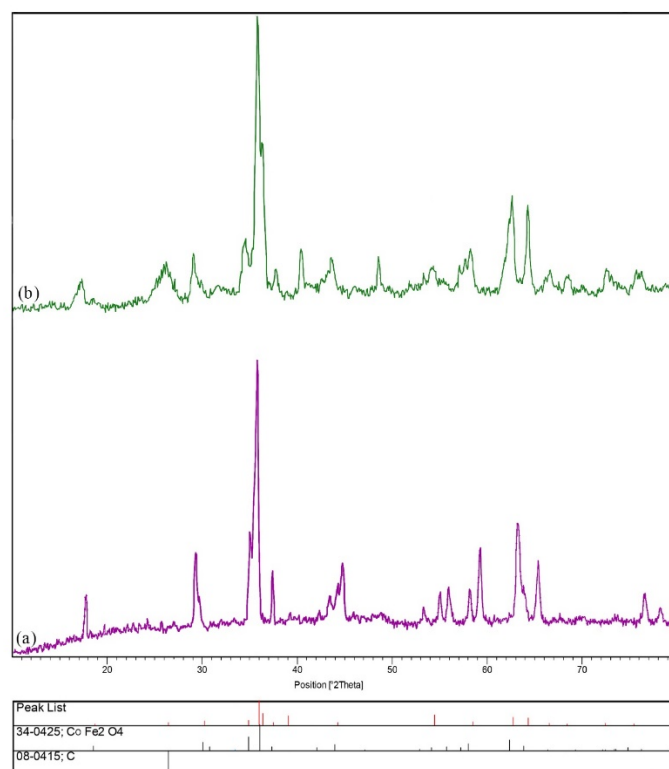


**Fig. 1.** XRD pattern of (a) CoFe<sub>2</sub>O<sub>4</sub> nanostructures and (b) CoFe<sub>2</sub>O<sub>4</sub>/MWCNT heterostructure

TEM images of CoFe<sub>2</sub>O<sub>4</sub>-MWCNT heterostructure shown in Fig. 2. According to this images rod-like structures show present MWCNT and sphere-like structures revealed present CoFe<sub>2</sub>O<sub>4</sub> nanostructure in the sample.

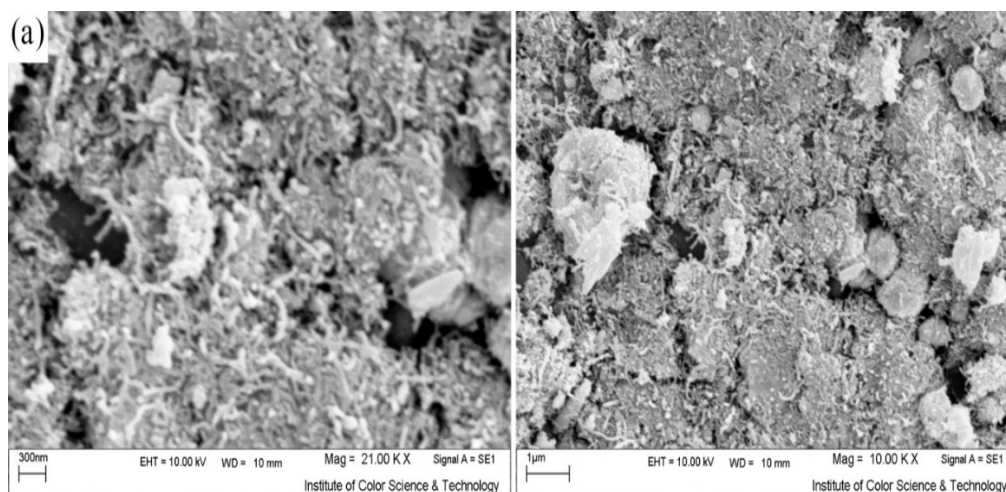


**Fig. 2.** SEM images of CoFe<sub>2</sub>O<sub>4</sub>/MWCNT heterostructure

FTIR spectrum of the prepared in present glucose is given in Fig. 6. The peaks around 573.25 and 403 cm<sup>-1</sup> confirmed stretching and bending vibrations of Fe-O and Co-O

(CoFe<sub>2</sub>O<sub>4</sub>) [54]. The peaks nearly 3430 and 1622 cm<sup>-1</sup> can be indicative of the absorbed moisture [55].

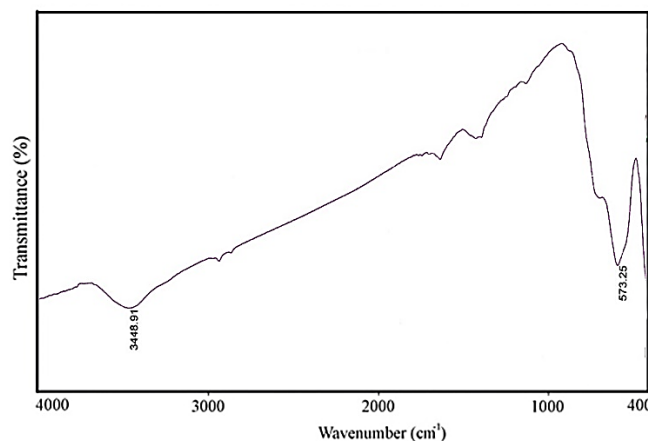


**Fig. 4.** FT-IR spectrum of as-synthesized CoFe<sub>2</sub>O<sub>4</sub> nanostructures

Fig. 4 shows room temperature hysteresis loops for the CoFe<sub>2</sub>O<sub>4</sub> annealed at 800 °C. The magnetic parameters such as saturation magnetization (M<sub>s</sub>), coercivity (H<sub>c</sub>), and remanent magnetization (M<sub>r</sub>) obtained from the hysteresis loops. Vibration samples magnetic showed a magnetization saturation (M<sub>s</sub>) was 5 emu/g with coercivity (H<sub>c</sub>) 2000 Oe and remanent magnetization (M<sub>r</sub>) 3 emu/g for CoFe<sub>2</sub>O<sub>4</sub>/MWCNT heterostructure.

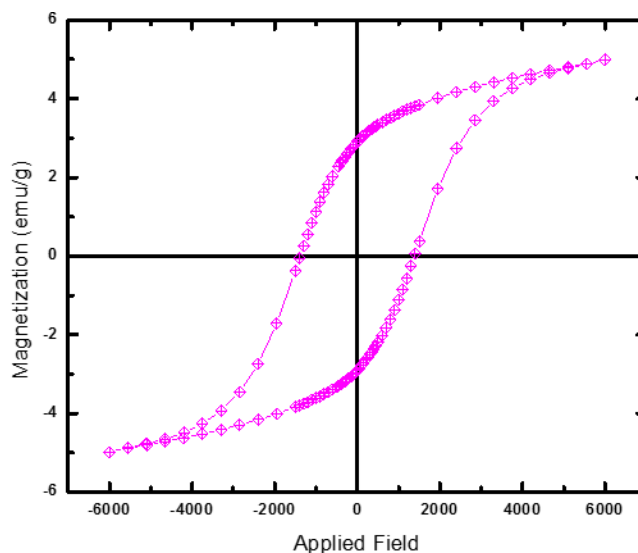


**Fig. 5.** VSM curves of CoFe<sub>2</sub>O<sub>4</sub> nanostructures

### 3.2. Study of the electrochemical behavior of ciprofloxacin at the surface of the modified electrode

The electrochemical behavior of 25 μM ciprofloxacin in a Briton Robinson buffer solution with pH=7 at the electrode surface was investigated using a cyclic voltammetry

techniques in the potential range of 0.5-1.2 V with a sweep velocity of 50 mV/s. In Fig. 6, voltammograms derived from the electrochemical behavior of ciprofloxacin at the surface of GC, MWCNT/GC and CoFe<sub>2</sub>O<sub>4</sub>-MWCNT/GC electrodes are presented. The ciprofloxacin drug at the surface of the GC electrode has an oxidation peak at the potential of 0.97 volts with a current of 1.6  $\mu$ A. The drug at the surface of the MWCNT/GC electrode has an oxidation peak potential at the potential of 0.92 V with a current of 5.5  $\mu$ A, which has a higher oxidation current than the unmodified electrode and its oxidation occur in lower potential. Finally, 25  $\mu$ M of ciprofloxacin in Briton Robinson buffer solution with pH=7 at the surface of CoFe<sub>2</sub>O<sub>4</sub>-MWCNT/GC electrode has more current than the other two electrodes, also oxidation peak potential of ciprofloxacin at the surface of this electrode has not changed relative to the MWCNT/GC electrode. An increase in the current rate for the GC and MWCNT/GC electrodes indicates that the CoFe<sub>2</sub>O<sub>4</sub>-MWCNT/GC electrode has a good electrocatalytic activity for ciprofloxacin, which is due to the synergistic effect of these two compounds.

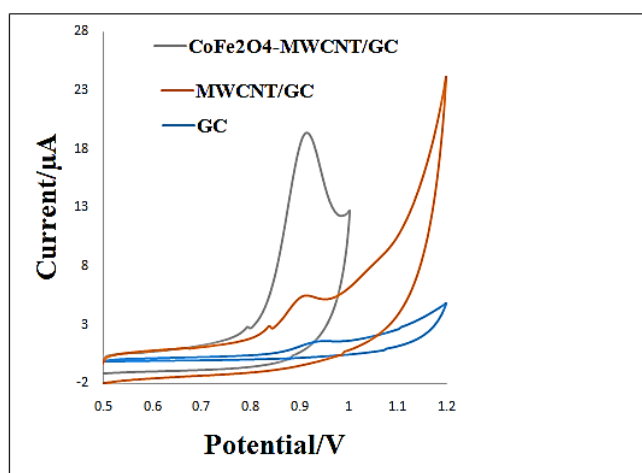


**Fig. 6.** The plot of CV for ciprofloxacin solution 25  $\mu$ M in Briton Robinson buffer solution with pH=7 at the surface of GC electrode, MWCNT/GC electrode and CoFe<sub>2</sub>O<sub>4</sub>-MWCNT/GC electrode at the scan rate of 50 mV/s

### 3.3. Study of the effects of scan rate

From the effect of the potential scan rate on electrochemical properties of CoFe<sub>2</sub>O<sub>4</sub>-MWCNT/GC electrode, the absorption or diffusion of the electrochemical reaction of ciprofloxacin can be obtained at the surface of CoFe<sub>2</sub>O<sub>4</sub>-MWCNT/GC electrode. For this purpose, voltammograms at scan rates ranging from 10-300 mV/s from a 25  $\mu$ M solution of ciprofloxacin in a Briton Robinson buffer solution with pH=7 are recorded and the results are shown in Fig. 7. As shown in Fig. 7a, with increasing scan rate, the current oxidation peak is increased and the potential shifted to the positive direction, which indicates the irreversibility

of the electrochemical reaction of ciprofloxacin at the electrode surface. The existence of dependence between the peak current and square root of scan rate indicating the oxidation ciprofloxacin is diffusion controlled behavior at the electrode surface (Fig. 7b). In order to obtain the electron transfer coefficient ( $\alpha$ ), the data of log current- potential curves were used. In this chart, the gradient of the graph for an oxidative reaction is equivalent to equation (1) [56].

$$\text{Slope} = 2.303RT / (1 - \alpha)nF \quad (1)$$

In this equation,  $R$  is universal gas constant,  $F$  is Faraday constant and the temperature is  $T$ . Thus, the electron transfer coefficient for ciprofloxacin is equal to 0.67 ( $n=2$ ).

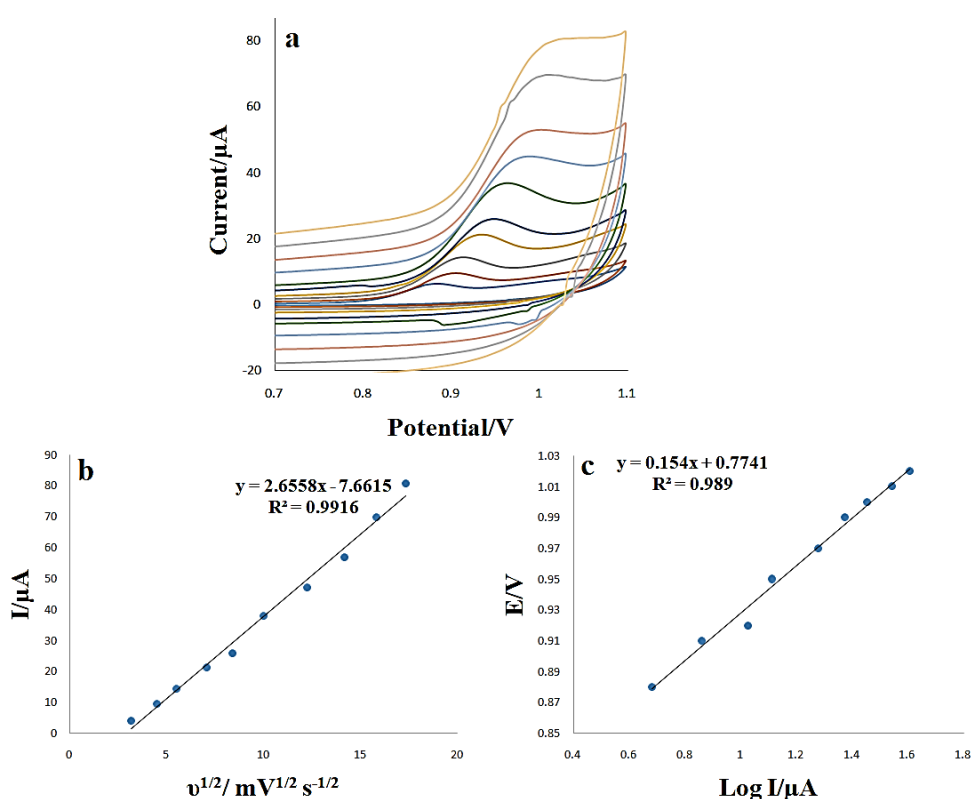


**Fig. 7.** a) CVs of the solution of ciprofloxacin 25  $\mu\text{M}$  in a Britton Robinson buffer solution with  $\text{pH}=7$  at the  $\text{CoFe}_2\text{O}_4\text{-MWCNT/GC}$  surface at different potential scan rates; b) The plot of anodic current versus root square of potential scan rate; c) The plot of Tafel obtained from the recorded current-potential curve at the scan rate of 10-300  $\text{mV/s}$

### 3.4. Effect of pH

The pH effect of buffer solution for better sensitivity of ciprofloxacin drug measurement was investigated in the pH range of 2-9 in the presence of 25  $\mu\text{M}$  of drug. The resulting voltammograms are shown in Fig. 8. The results indicate that the highest current is related to  $\text{pH}=7$ , therefore it was used as an optimal pH. The linear gradient of the potential curve vs.



pH is equal to 0.060, which suggests it's following from Nernst equation, so the number of electrons and protons involved in the ciprofloxacin oxidation reaction are equal. The oxidation mechanism, as reported in the papers, is presented in Schematic 1.

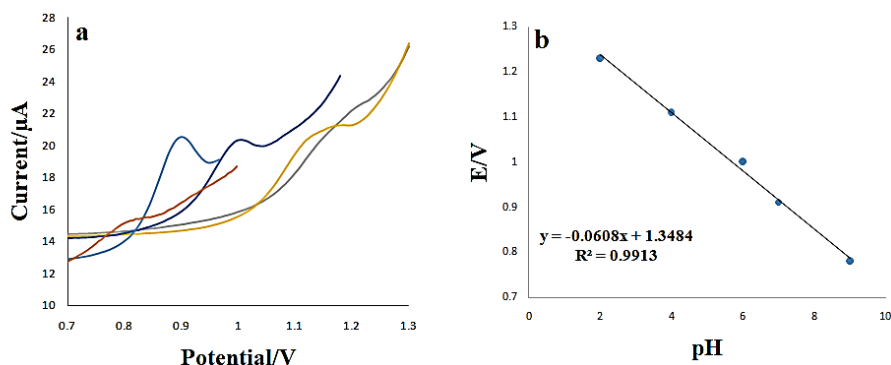


**Fig. 8.** a) The plot of CV of the oxidation 25 $\mu$ M of ciprofloxacin at the CoFe<sub>2</sub>O<sub>4</sub>-MWCNT/GC surface to check the effect of pH (from right to left 2, 4, 6, 7, 9); b) The plot of  $E_{pa}$  against the pH

### 3.5. Differential pulse Voltammetry

Differential pulse Voltammetry technique was used to analyze various amounts of ciprofloxacin in a Briton Robinson buffer solution with pH=7. The differential pulse voltammograms along with the resulting calibration graph are shown in Fig. 9. The oxidation peak currents of ciprofloxacin were linear with its concentrations in two range of 0.1-1  $\mu$ M and 1-30  $\mu$ M, and the limit of detection is also equal to 0.036  $\mu$ M according to the equation of  $LOD=3S/m$ .

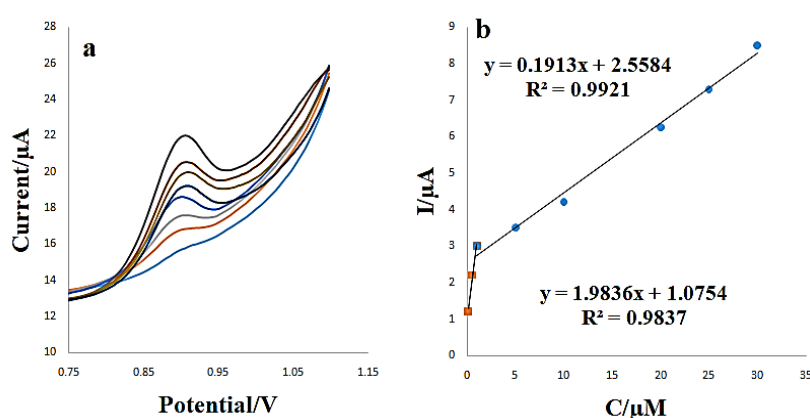


**Fig. 9.** a) DPVs of different concentrations of ciprofloxacin in the range 0.1 to 30  $\mu$ M Briton Robinson buffer solution with pH=7 at the CoFe<sub>2</sub>O<sub>4</sub>-MWCNT/GC electrode; b) The plot of the linear calibration curve for peak current  $I_{p,a}$  versus the ciprofloxacin concentration

Table 1 compares the other electrochemical techniques to determine ciprofloxacin. From the comparison of the modified electrode with Table 1, it can be concluded that the desired electrode has the ability to determine the low levels of this drug. As can be seen in this table, the proposed electrode exhibits more appropriate analytical properties for example low detection limit and wide linear dynamic ranges for the electrochemical determination of ciprofloxacin. So it is displayed that the CoFe<sub>2</sub>O<sub>4</sub>-MWCNT/GC electrode was a good choice for electrochemical sensing of ciprofloxacin.

**Table 1.** Comparison of the Electrochemical Methods for determining the ciprofloxacin

Electrode	Background electrolyte	Method	Dynamic range (μM)	LOD (μM)	Ref.
Boron-doped diamond electrode	Britton Robinson buffer (pH 4)	Differential pulse Voltammetry	0.74-20	0.6	[27]
DNA/GC electrode	Acetate buffer solution (pH 5)	Differential pulse Voltammetry	1-10	0.11	[29]
MWCNT/GC electrode	Phosphate buffer solution (pH 7)	Linear sweep voltammetry	2-780	0.9	[30]
Boron-doped diamond electrode	Britton Robinson buffer (pH 7)	Square-wave voltammetry	0.5-60	0.4	[57]
CoFe <sub>2</sub> O <sub>4</sub> -MWCNT/GC electrode	Britton Robinson buffer (pH 7)	Differential pulse Voltammetry	0.1-20	0.036	This work

#### 4. CONCLUSION

Pure CoFe<sub>2</sub>O<sub>4</sub> spherical-like have been synthesized by a sol-gel method using glucose as a template. It is nontoxic, cost-effective, green, and is environmentally friendly. Therefore, magnetic properties of CoFe<sub>2</sub>O<sub>4</sub>/MWCNT heterostructure showed the ferrimagnetic with high magnetic saturation. SEM images and XRD analysis of the products indicated that sphere-like nanoparticles with average size of 60 nm and crystal size 18 nm. The modified electrode could well analyze the low levels of ciprofloxacin in the aqueous solution, which had the highest sensitivity at pH=7. At the surface of this electrode show two wide linear dynamic range of 0.1-1 μM and 1-30 μM with limit of detection of 0.036 μM. The electrocatalytic ability of the CoFe<sub>2</sub>O<sub>4</sub>-MWCNT/GC electrode can be attributed to the synergistic effect of the carbon structure and the nanoparticle used within it.

**REFERENCES**

- [1] M. Aghazadeh, *Mater. Lett.* 211 (2018) 225.
- [2] S. M. Hosseinpour-Mashkani, and A. Sobhani-Nasab, *J. Mater. Sci. Mater. Electron.* 27 (2016) 3240.
- [3] S. M. Pourmortazavi, Z. Marashianpour, M. Sadeghpour Karimi, M. Mohammad-Zadeh, *J. Mol. Struct.* 1099 (2015) 232.
- [4] F. Ahmadi, M. Rahimi-Nasrabadi, A. Fosooni, and M. Daneshmand. *J. Mater. Sci. Mater. Electron.* 27 (2016) 9514.
- [5] A. Sobhani-Nasab, M. Behpour, M. Rahimi-Nasrabadi, F. Ahmadi, and S. Pourmasoud, *J. Mater. Sci. Mater. Electron.* 30 (2019) 5854.
- [6] A. Sobhani Nasab, S. Pourmasoud, F. Ahmadi, M. Wysokowski, T. Jesionowski, H. Ehrlich, and M. Rahimi-Nasrabadi, *Mater. Lett.* 238 (2019) 159.
- [7] A. Sobhani-Nasab, M. Rangraz-Jeddy, A. Avanes, and M. Salavati-Niasari, *J. Mater. Sci. Mater. Electron.* 26 (2015) 9552.
- [8] S. M. Pourmortazavi, M. Taghdiri, N. Samimi, and M. Rahimi-Nasrabadi, *Mater. Lett.* 121 (2014) 5.
- [9] A. Sobhani-Nasab, and M. Behpour, *J. Mater. Sci. Mater. Electron.* 27 (2016) 1191.
- [10] M. Rahimi-Nasrabadi, M. Behpour, A. Sobhani-Nasab, and M. Rangraz Jeddy, *J. Mater. Sci. Mater. Electron.* 27 (2016) 11691.
- [11] M. Rahimi-Nasrabadi, M. Behpour, A. Sobhani-Nasab, and S. M. Hosseinpour-Mashkani, *J. Mater. Sci. Mater. Electron.* 26 (2015) 9776.
- [12] M. Salavati-Niasari, F. Soofivand, A. Sobhani-Nasab, M. Shakouri-Arani, M. Hamadanian, and S. Bagheri, *J. Mater. Sci. Mater. Electron.* 28 (2017) 14965.
- [13] S. M. Hosseinpour-Mashkani, A. Sobhani-Nasab, and M. Mehrzad, *J. Mater. Sci. Mater. Electron.* 27 (2016) 5758.
- [14] A. Sobhani-Nasab, M. Behpour, M. Rahimi-Nasrabadi, F. Ahmadi, and S. Pourmasoud, *J. Mater. Sci. Mater. Electron.* 30 (2019) 5854.
- [15] S. M. Hosseinpour-Mashkani, and A. Sobhani-Nasab, *J. Mater. Sci. Mater. Electron.* 27 (7) (2016) 7548.
- [16] Y. Ding, Y. Yang, and H. Shao, *Solid State Ion.* 217 (2012) 27.
- [17] W. Ponhan, and S. Maensiri, *Solid State Sci.* 11 (2009) 479.
- [18] J. Feng, L. Su, Y. Ma, C. Ren, Q. Guo, and X. Chen, *Chem. Eng. J.* 221 (2013) 16.
- [19] F. Qi, W. Chu, and B. Xu, *Chem. Eng. J.* 284 (2016) 28.
- [20] R. C. Wu, J. H. Qu, and H. He, *Appl. Catal. B* 48 (2004) 49.
- [21] S. M. Peymani-Motlagh, A. Sobhani-Nasab, M. Rostami, H. Sobati, M. Eghbali-Arani, M. Fasihi-Ramandi, M. R. Ganjali, and M. Rahimi-Nasrabadi, *J. Mater. Sci. Mater. Electron.* 30 (2019) 6902.

- [22] R. Sato Turtelli, G.V. Duong, W. Nunes, R. Grössinger, and M. Knobel, *J. Magn. Mater.* 320 (2008) 339.
- [23] D. Q. Wu, F. Zhang, H. W. Liang, and X. L. Feng, *Chem. Soc. Rev.* 41 (2012) 6160.
- [24] M. J. Allen, V. C. Tung, and R. B. Kaner, *Chem. Rev.* 110 (2009) 132.
- [25] J. H. Kim, H. Kim, and H. J. Sohn, *Electrochem. Commun.* 7 (2005) 557.
- [26] H. L. Liu, *Int. J. Electrochem. Sci.* 8 (2013) 2204.
- [27] K. Cinková, D. Andrejčáková, and L. Švorc, *Acta Chimica Slovaca* 9 (2016) 146.
- [28] M. Paal, M. Zoller, C. Schuster, M. Vogeser, and G. Schütze, *J. Pharm. Biomed. Anal.* 152 (2018) 102.
- [29] N. Diab, I. Abu-Shqair, R. Salim, and M. Al-Subu, *Int. J. Electrochem. Sci.* 9 (2014) 1771.
- [30] M. Rahimi-Nasrabadi, S. M. Pourmortazavi, M. Aghazadeh, M. R. Ganjali, M. Sadeghpour Karimi, and P. Norouzi, *J. Mater. Sci. Mater. Electron.* 28 (2017) 9478.
- [31] M. Rahimi-Nasrabadi, V. Pourmohamadian, M. Sadeghpour Karimi, H. R. Naderi, M. A. Karimi, K. Didehban, and M. R. Ganjali, *J. Mater. Sci. Mater. Electron.* 28 (2017) 12391.
- [32] M. Rahimi-Nasrabadi, S. M. Pourmortazavi, Z. Rezvani, K. Adib, and M. R. Ganjali, *Mater. Manuf. Processes* 30 (2015) 34.
- [33] M. Rahimi-Nasrabadi, *J. Mater. Sci. Mater. Electron.* 28 (2017) 2200.
- [34] A. Khoshroo, L. Hosseinzadeh, A. Sobhani-Nasab, M. Rahimi-Nasrabadi, and H. Ehrlich, *J. Electroanal. Chem.* 823 (2018) 61.
- [35] J. Hassanzadeh, B. Rezaei Moghadam, A. Sobhani-Nasab, F. Ahmadi, and M. Rahimi-Nasrabadi, *Spectrochim. Acta Part A* 214 (2019) 451.
- [36] M. Rahimi-Nasrabadi, H. R. Naderi, M. Sadeghpour Karimi, F. Ahmadi, and S. M. Pourmortazavi, *J. Mater. Sci. Mater. Electron.* 28 (2017) 1877.
- [37] J. Amania, M. Malekia, A. Khoshroo, A. Sobhani-Nasabb, M. Rahimi-Nasrabadi, *Anal. Biochem.* 548 (2018) 53.
- [38] M. Aghazadeh, I. Karimzadeh, and M. R. Ganjali, *J. Mater. Sci.: Mater. Electron.* 28 (2017) 13532.
- [39] M. Rahimi-Nasrabadi, F. Ahmadi, and M. Eghbali-Arani, *J. Mater. Sci. Mater. Electron.* 27 (2016) 11873.
- [40] S. M. Hosseinpour-Mashkani, M. Ramezani, A. Sobhani-Nasab, and M. Esmaeili-Zare, *J. Mater. Sci. Mater. Electron.* 26 (2015) 6086.
- [41] M. Rahimi-Nasrabadi, F. Ahmadi, and A. Fosooni, *J. Mater. Sci. Mater. Electron.* 28 (2017) 537.
- [42] M. Ramezani, A. Sobhani-Nasab, and S. M. Hosseinpour-Mashkani, *J. Mater. Sci. Mater. Electron.* 26 (2015) 4848.

- [43] M. Ramezani, S. M. Hosseinpour-Mashkani, A. Sobhani-Nasab, and H. Ghasemi Estarki, *J. Mater. Sci. Mater. Electron.* 26 (2015) 7588.
- [44] M. Eghbali-Arani, A. Sobhani-Nasab, M. Rahimi-Nasrabadi, and S. Pourmasoud, *J. Electron. Mater.* 47 (2018) 3757.
- [45] S. S. Hosseinpour-Mashkani, and A. Sobhani-Nasab *J. Mater. Sci. Mater. Electron.* 28 (2017) 16459.
- [46] M. Rahimi-Nasrabadi, M. Rostami, F. Ahmadi, A. F. Shojaie, and M. D. Rafiee, *J. Mater. Sci. Mater. Electron.* 27 (2016) 11940.
- [47] S. M. Hosseinpour-Mashkani, and A. Sobhani-Nasab, *J. Mater. Sci. Mater. Electron.* 28 (2017) 4345.
- [48] A. Sobhani-Nasab, and M. Behpour *J. Mater. Sci. Mater Electron.* 27 (2016) 11946.
- [49] S. M. Hosseinpour-Mashkani, M. Maddahfar, and A. Sobhani-Nasab, *J. Electron. Mater.* 45 (2016) 3612.
- [50] H. Kooshki, AliSobhani-Nasab, M. Eghbali-Arani, F. Ahmadi, V. Ameri, and M. Rahimi-Nasrabadi, *Separat. Purificat. Technol.* 18 (2019) 873.
- [51] M. Salavati-Niasari, F. Soofivand, A. Sobhani-Nasab, M. Shakouri-Arani, and S. Bagheri, *Adv. Powder Technol.* 27 (2016) 2066.
- [52] F. Ahmadi, M. Rahimi-Nasrabadi, A. Fosooni, and M. Daneshmand, *J. Mater. Sci. Mater. Electron.* 27 (2016) 9514.
- [53] M. Maddahfar, M. Ramezani, M. Sadeghi, and A. Sobhani-Nasab, *J. Mater. Sci. Mater. Electron.* 26 (2015) 7745.
- [54] F. Sedighi, M. Esmaili-Zare, A. Sobhani-Nasab, and M. Behpour, *J. Mater. Sci. Mater. Electron.* 29 (2018) 13737.
- [55] S. M. Asgarian, S. Pourmasoud, Z. Kargar, A. Sobhani-Nasab, and M. Eghbali-Arani, *Mater. Res. Express* 6 (2018) 015023.
- [56] A. Bard, and L. Faulkner, *Electrochem. Method.* 2 (2001) 482.
- [57] Garbellini, Gustavo Stoppa, Romeu C. Rocha-Filho, and O. Fatibello-Filho, *Anal. Method.* 7 (2015) 3411.